

EFFECTS OF SOIL SPATIAL VARIABILITY ON DYNAMIC BEHAVIOR ON SHEET-PILE SUPPORTED GROUND

Hyuk Kee HONG¹, Yoshikasu TANAKA², Kyohei UEDA³

¹Non-member of JSCE, Research student, Disaster Prevention Research Institute, Kyoto University
(Gokasho, Uji, Kyoto 611-0011, Japan)

E-mail: hyukkee.hong.37e@st.kyoto-u.ac.jp

²Member of JSCE, Doctoral researcher, Disaster Prevention Research Institute, Kyoto University
(Gokasho, Uji, Kyoto 611-0011, Japan)

E-mail: tanaka.yoshikazu.5m@kyoto-u.ac.jp

³Member of JSCE, Assistant Professor, Disaster Prevention Research Institute, Kyoto University
(Gokasho, Uji, Kyoto 611-0011, Japan)

E-mail: ueda.kyohei.2v@kyoto-u.ac.jp

The finite element method using the deterministic model is generally used to predict soil liquefaction due to earthquakes. However, the deterministic model does not consider the intrinsic spatial variability of natural ground. This means that a probabilistic approach is necessary because it is impossible to investigate all soil properties of the target site. Therefore, research on how spatial variability affects dynamic behavior is required. In this study, liquefaction behavior was compared between stochastic models that applied spatial variability to the soil deposit and deterministic models. Here, the variable of spatial variability is a relative density, and both models have the same mean value with a variation coefficient of 0.1. The analyzed model is the saturated sandy soil deposit with sheet-pile. According to the results of stochastic models, the horizontal displacement of the sheet-pile and backfill soil were comparable with deterministic model. However, a large difference from the deterministic model was shown in the pore water pressure results of the stochastic models. Especially, it is significant in the soil affected by the sheet-pile displacement. As a result, the spatial variability on dynamic behavior is significant on pore water pressure, not in displacement.

Key words: liquefaction, finite element method, spatial variability, pore water pressure, sheet-pile displacement

1. INTRODUCTION

The research on liquefaction, the modeling through the finite element method, is widely used in numerical simulation. However, numerical simulation is generally conducted in a deterministic model. In contrast, the actual ground has spatial variability even in the case of the site is considered to be a homogeneous area.

The dynamic behavior such as earthquake, the spatial variability of the soil properties causes a difference in the predicted response¹⁾. Even if sampling and measuring the soil properties can be a solution. However, sampling at every location is impractical, and the measurement error may not be able to get exact properties²⁾. Therefore, a probabilistic analysis is required since the soil properties of the target site have uncertainty.

According to mentioned above problem,

Liquefaction Experiments and Analysis Projects (LEAP) is working on verifying the experimental variation and finding a calibration method. The LEAP project focuses on comparing the model experiment with numerical simulation about the dynamic response of the liquefiable sand deposit³⁾.

In this study, as an extension of the LEAP project, the LEAP-2020-RPI model is applied, which has a sheet-pile. By the motivation of the LEAP project, the theme of this research is an investigation of the spatial variability effects on dynamic behavior. Therefore, it is conducted that the dynamic analysis on 10 cases of the stochastic model base on the Gaussian field. As the relative density is the variable of the Gaussian field, it is created randomly with the same mean value and standard deviation on the normal distribution. Also, the deterministic models are 3 cases with mean relative density ($\mu = D_r/60$) and both standard deviation with 0.1 of variation

coefficient ($\mu \pm \sigma = 60 \pm 6$). Both cases with 0.1 of variation coefficient consist the range (D_r 54 and D_r 66) of the prediction as a criterion of result examination.

The investigation of the spatial variability effects is focused on the displacement and the pore water pressure. The numerical analysis program is the finite element analysis program of liquefaction process FLIP. Referring method in this study is according to Vargas et al.⁴⁾. it is a two-dimensional

nonlinear finite element analysis for verifying the effect of dynamic response on liquefiable heterogeneity sand deposit. Also, it is based on the Monte Carlo simulation method according to the method proposed by Popescu et al.⁵⁾, and the nonlinearity of the soil is expressed using a strain space multiple mechanism model^{6), 7)}. Furthermore, this research considers effects on the sheet-pile model, whereas the model of Vargas et al. is horizontally layered ground.

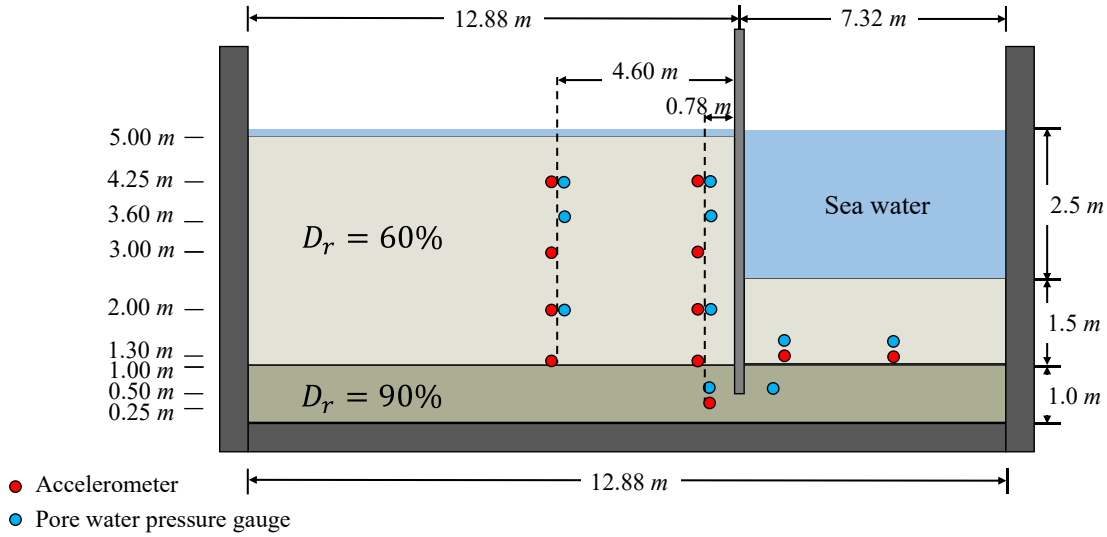


Fig. 1 schematic centrifuge test model with prototype scale referred to the LEAP-2020-RPI

2. SOIL PROPERTIES MODELING

(1) Model parameters

The material of the LEAP-2020-RPI is Ottawa F65 sand, and Fig. 1 shows the schematic model. According to Fig. 1, the different parameter is applied due to the relative density difference. Each layer has 60% and 90% of relative density. Also, this model is given model from the LEAP-2020-RPI.

Table 1 and Table 2 represent the model parameters for the characteristic of the deformation and dilatancy, respectively. Especially, as shown in Table 2, dilatancy parameters have been set in a 60% relative density layer. However, the 90% relative density layer has not been established for dilatancy parameters. This shows the 60% relative density layer is a liquefiable layer, whereas the 90% relative

density layer is the non-liquefiable layer. Even though the dense layer can liquefy in the actual soil deposit, the modeling was conducted to simplify the comparison of the spatial variability effect for the liquefiable layer. Also, the spatial variability is applied only to the backfill soil on the left side of the sheet-pile (see Fig. 2).

Table 1 Model parameters for deformation characteristics			
Parameter designation		D_r 60	D_r 90
P_a	Confining pressure (kPa)	73.5	
G_{ma}	Shear modulus (kPa)	54,118	113,605
K_{L/U_c}	Bulk modulus (kPa)	14,113	296,264
ρ_t	Mass density (t/m^3)	2.092	
n	Porosity	0.470	0.419
ϕ_f^{PS}	Internal friction angle ($^\circ$)	35.94	48.0
H_{max}	Maximum damping constant	0.24	

Table 2 Model parameters for dilatancy			
Parameter designation		D_r 60	D_r 90
ϕ_p	Phase transformation angle ($^\circ$)	28.0	-
ε_d^{cm}	Limit of contractive component (negative dilatancy)	0.2	-
$r_{\varepsilon_d^c}$	Negative dilatancy control parameter	1.996	-
r_{ε_d}	Positive and negative dilatancy control parameter	1.136	-
q_1	Initial phase of EPWP control parameter in negative dilatancy	1.0	-

q_2	Final phase of EPWP control parameter in negative dilatancy	0.956	-
l_k	Power index of bulk modulus of EPWP dissipation parameter	2	-
r_K	Bulk modulus reduction factor	0.5	-
S_1	Small positive number to avoid zero confining pressure	0.005	-
c_1	Parameter controlling elastic range for contractive component	1.874	-
q_4	Adjust parameter of contractive component in liquefaction	1.0	-
q_{us}	Undrained shear strength in steady state	-	-

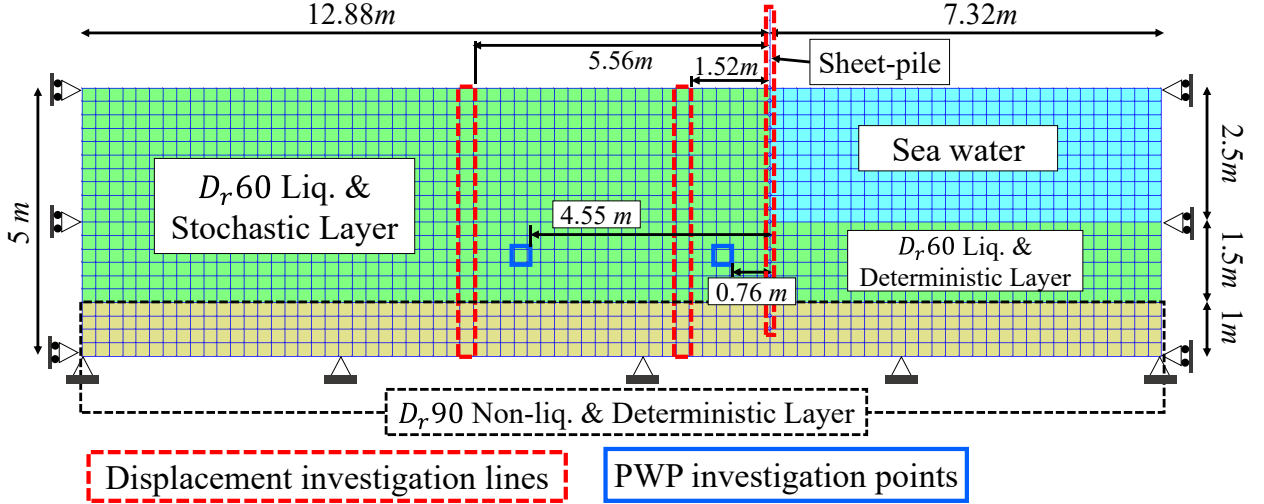


Fig. 2 Mesh model by finite element method program FLIP and description of each layer

(2) Modeling of spatial variability models

Base on the mesh model shown in Fig. 2, Gaussian random variables used of the stochastic layer are based on the spectral density function of two-dimensional stochastic fields. The spectral density function is shown in equation (1). The details in Ref⁽⁴⁾

$$\sigma^2 \cdot \frac{d_x d_y}{4\pi} \exp \left\{ - \left(\frac{d_x^2}{4} \kappa_x^2 + \frac{d_y^2}{4} \kappa_y^2 \right) \right\} \quad (1)$$

Where $\kappa = (\kappa_x, \kappa_y)^T$ is a wave number vector. In equation (1), σ is the standard deviation of variational in x and y -axis. Also, referring to Nadim et al.⁽⁸⁾, $d_x=10.0m$ and $d_y=1.0m$ were used.

Also, by assuming the zero for the mean value, the spectral density function of random process⁽⁸⁾ is derived by equation (2).

$$f(x, y) = \sqrt{2} \sum_{k=1}^{K_x} \sum_{l=1}^{K_y} A_{kl} \times \left[\cos(\kappa_{xk}x + \kappa_{yl}y + \Phi_{kl}^{(1)}) + \cos(\kappa_{xk}x - \kappa_{yl}y + \Phi_{kl}^{(2)}) \right] \quad (2)$$

Where, Φ_{kl} is an independent random phase angle distributed with uniformity between 0 and 2π . K_x and K_y is the division number for calculating wave number in x and y direction, respectively. Here, the A_{kl} is the following equation (3)

$$A_{kl} = \sqrt{2S(\kappa_{xk}, \kappa_{lk}) \Delta \kappa_x \Delta \kappa_y} \quad (3)$$

where, $\Delta \kappa$ is an incremental vector of wave number. The detail is in Ref⁽⁴⁾.

As a result, the stochastic field spatial variability is following equation (4).

$$F(x, y) = f_m + f(x, y) \quad (4)$$

Spatial variability of the stochastic field is determined by the sum of the mean value (f_m) and the estimated random process $f(x, y)$. Also, F is the spatial distribution which is stochastic variables of the soil properties heterogeneity. According to the above equations, the spatial distribution is shown in Fig. 3. Also, Fig. 4 shows that the relative density is expressed as the spatial distribution of the stochastic variable, and Fig. 5 shows the correlation function.

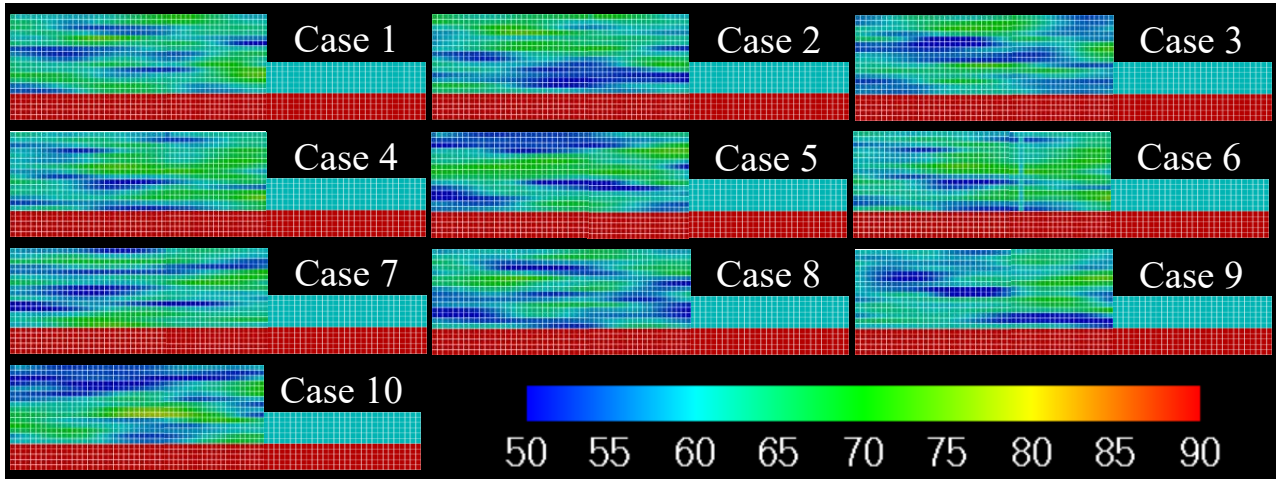


Fig. 3 Spatial distribution of relative density for Gaussian stochastic fields

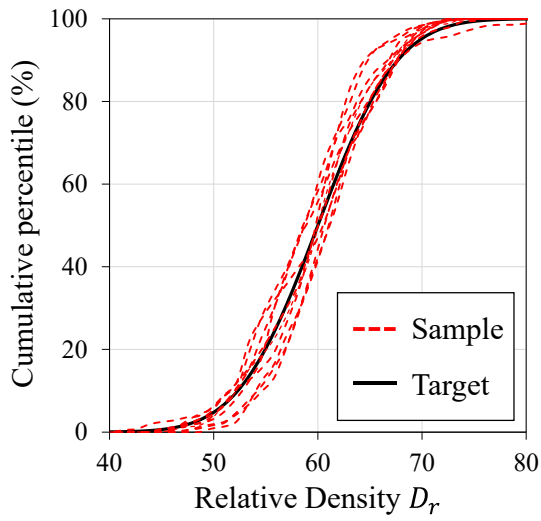


Fig. 4 Cumulative distribution function for relative density

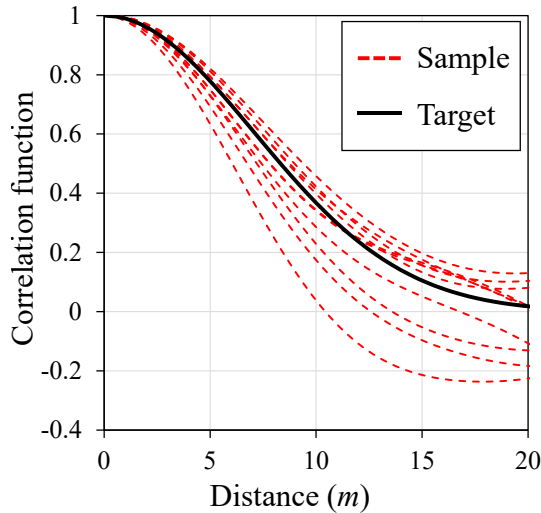


Fig. 5 Correlation function for relative density

3. NUMERICAL SIMULATION PROCEDURE

Fig. 2 shows the mesh and boundary condition by finite element analysis program FLIP. In modeling,

2,999 total elements are created for 20 rows and 80 columns. The total elements are including 1,310 pore water elements and 26 joint elements. The parameters for joint elements are shown in Table. 3. Joint elements parameters are activated for landward and seaward. Also, the bottom of the sheet-pile joint element modeled as a free condition for x and y -direction.

Table. 3 Parameters for joint elements		
Symbol	Parameter designation	Value
ϕ_f	Friction angle ($^\circ$)	15
K_n	Initial vertical rigidity(kPa/m)	1.0E+6
K_s	Initial rigidity for shear direction(kPa/m)	1.0E+4

Referring the Vargas et al.⁴⁾, Fig. 6 shows the parameter identification of the finite element program of liquefaction process FLIP based on the SPT N value. The detailed explanation is Ref^{4), 7)}.

According to Fig. 7, the 1 Hz, 20 cycles, and peak ground acceleration (PGA) is $0.15g$ applied to the base as the input motion. Also, the input motion is given data from LEAP.

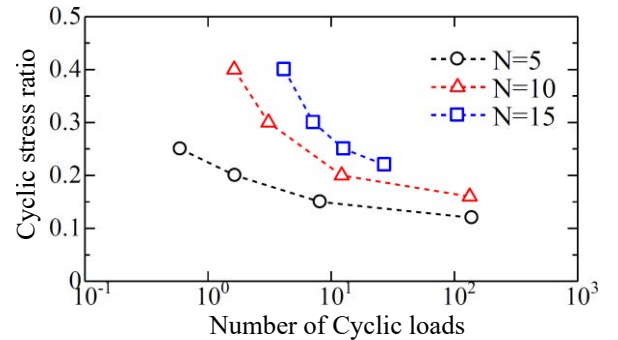


Fig. 6 Liquefaction resistance curve

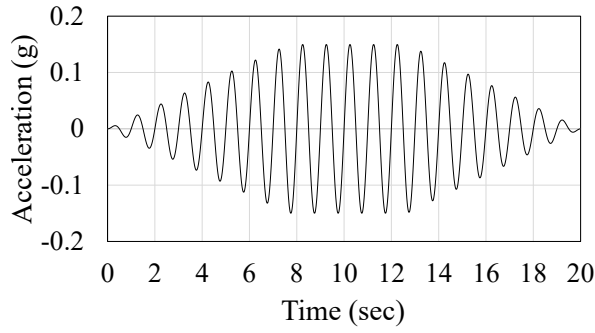


Fig. 7 Input ground motion

4. ANALYSIS RESULTS

(1) Lateral displacement of sheet-pile

Fig. 8 and Fig. 9 show the sheet-pile horizontal displacement of the deterministic and Gaussian stochastic models. Fig. 8 shows the after-shaking result of the horizontal displacement for elevation (investigation point; see Fig. 2). The result of Fig. 8 shows that the Gaussian stochastic model cases were evenly distributed in the standard deviation range of the deterministic models.

Also, Fig. 9 is the sheet-pile top horizontal displacement with time history. The displacement results after shaking (at 20 seconds), are the same as Fig. 8. Therefore, Gaussian stochastic models are distributed inside the standard deviation range of the deterministic model at the final. However, some stochastic model results are outside of the standard deviation range of the deterministic model during shaking. These differences from the standard deviation range significantly occur after the input motion shows peak ground acceleration (PGA). Furthermore, the average result value of the 10 cases for the Gaussian stochastic models (green line) is close to the $D_{r,60}(\mu)$ deterministic model result.

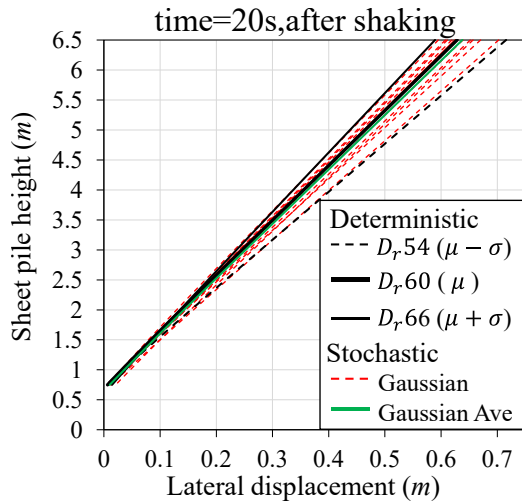


Fig. 8 Lateral displacement of sheet-pile

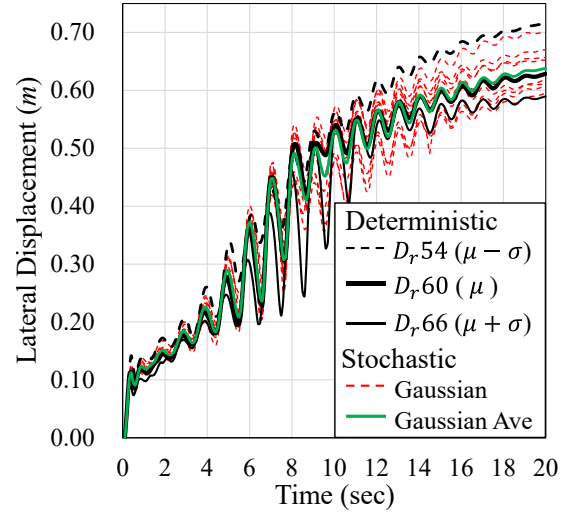


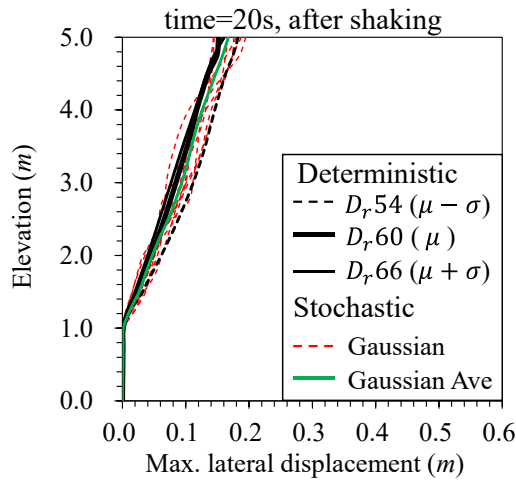
Fig. 9 Lateral displacement of sheet-pile top according to the time history

(2) Lateral displacement of backfill soil

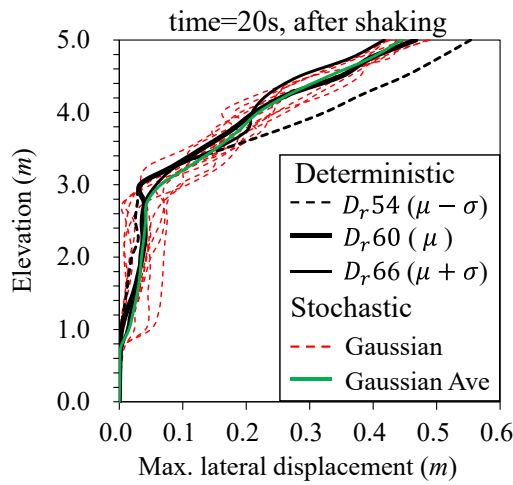
Fig. 10 shows the lateral displacement of the backfill soil. According to Fig. 2, the investigation lines are 5.56 m and 1.52 m to the left from the sheet-pile.

First, 5.56 m to the left from the sheet-pile, as shown in Fig. 10 (a), is a small enough effect of the sheet-pile displacement. Second, 1.52 m to the left from the sheet-pile is directly affected by the sheet-pile displacement, as shown in Fig. 10 (b).

Considering the model scale for horizontal length is 20.2 m, Fig. 10 (a) shows that spatial variability of relative density does not significantly affect displacement where far enough from sheet-pile. The most considerable difference outside from deterministic model standard deviation range is about 1 cm. Also, the case of the displacement at nearby the sheet-pile, as shown in Fig. 10 (b), shows a larger difference. There is almost a 5 cm difference at 4 m deep from the surface. However, this can also be assumed as a small difference, and determining a similar result with the $D_{r,60}(\mu)$ deterministic model is possible by considering the stochastic model's average result value for prediction.



(a) Left 5.6 m from the sheet-pile



(b) Left 1.5 m from the sheet-pile

Fig. 10 Lateral displacement of medium part of the backfill soil

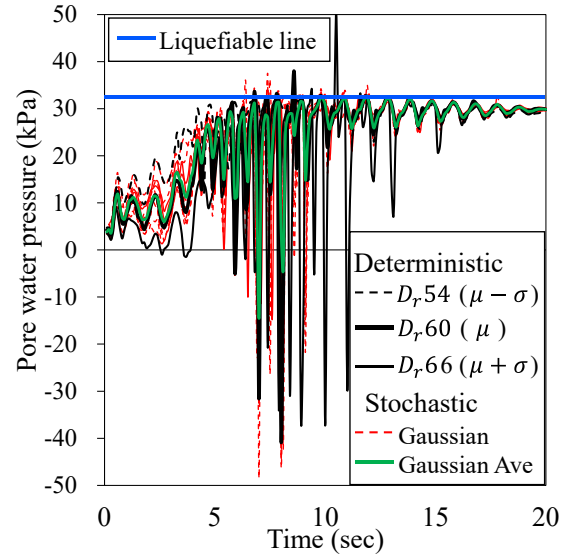
(3) Excess pore water pressure ratio

According to Fig. 2, the investigation point of the pore water pressure is 3 m depth from the surface. Also, Fig. 11 (a) and Fig. 11 (b) show the pore water pressure results for x-direction, 4.6 m, and 0.78 m away from the sheet-pile to the left, respectively (see Fig. 2).

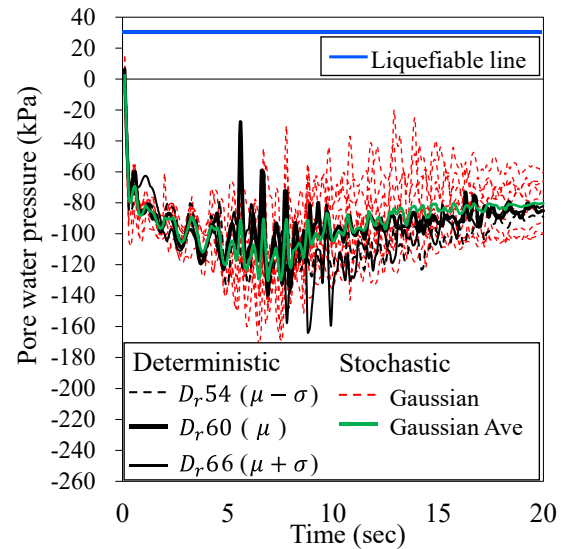
After shaking, Fig. 11 (a) shows that the Gaussian stochastic models show similar results to the $D_{r60} (\mu)$ of the deterministic model. However, the accumulation process has a large difference. This is considered the different spatial variability for each case affected by the dynamic motion.

Fig. 11 (b) shows a significant difference in the results of stochastic models, whereas there is no

large difference in the case of the deterministic models. However, unlike Fig. 11 (a), sheet-pile displacement effects at Fig. 11 (b) investigation point. This leads to the volume change of the soil due to the constraint force decrease. Also, the decrease of the constraint force by sheet-pile displacement induced the negative value of pore water pressure. Therefore, the result variation by the spatial variability effect is significant, especially when there is a volume change of soil. Fig. 12 shows the distribution of the pore water pressure after-shaking for every case.



(a) Left 4.55 m from the sheet-pile



(b) Left 0.76 m from the sheet-pile

Fig. 11 Time history of maximum EPWP ratio.

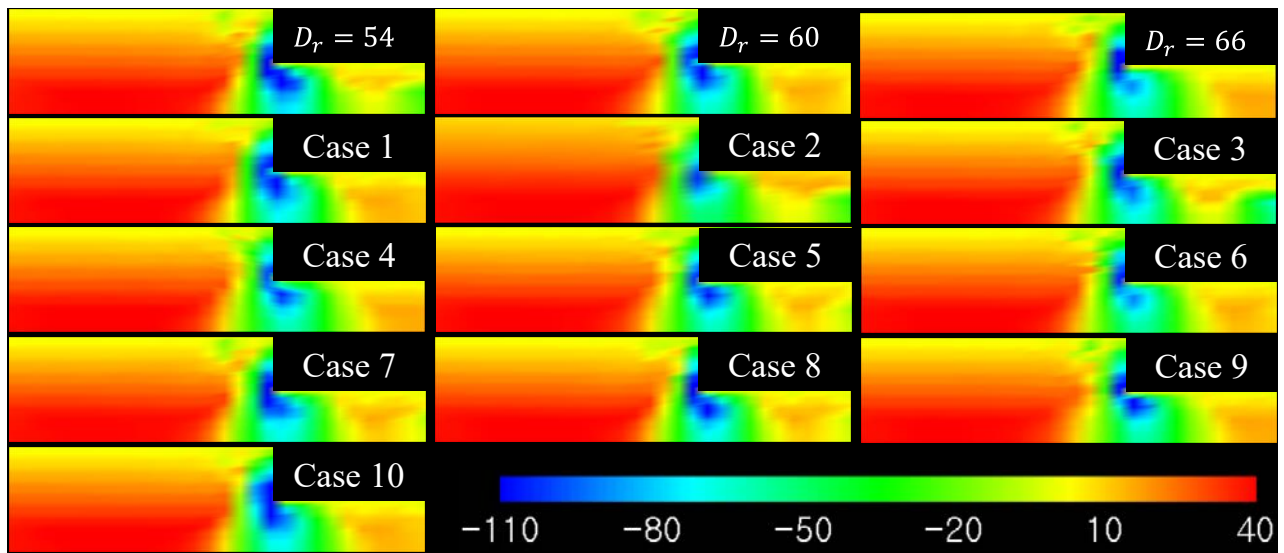


Fig. 12 Distribution of pore water pressure after shaking

5. CONCLUSION

As an extension of the LEAP-2020-RPI, the effect of spatial variability on dynamic behavior is investigated by comparing deterministic and stochastic models to verify experimental variation. The spatial variability is based on the Gaussian stochastic field, and the variable is relative density. Also, the variation coefficient for the mean value is 0.1.

First, the spatial variability is not significant for the horizontal displacement. For the displacement of the sheet-pile top, the results of the stochastic models were within the standard deviation range of the deterministic homogeneous models. Even though for the backfill soil displacement, the 5 cm difference from range in some cases is not significant considering that the horizontal length of the model is 20.2 m. Therefore, spatial variability should be regarded for prediction, but not highly important. Also, the variation coefficient of 0.1 can cover the displacement results.

Second, the spatial variability is significant for the pore water pressure. In the case of a sufficiently far distance from the sheet-pile, there is a large difference during shaking, even the after-shaking result covered by the standard deviation range. In addition, the standard deviation range cannot cover the pore water pressure nearby the sheet-pile displacement due to the volume change of soil. Therefore, a variation coefficient of 0.1 is not enough in the case of the pore water pressure.

REFERENCES

- 1) Montgomery, J. and Boulanger, R. W.: Effects of Spatial Variability on Liquefaction-Induced Settlement and Lateral Spreading, *Journal of Geotechnical and Geoenvironmental Engineering*, 2016 ([http://dx.doi.org/10.1061/\(ASCE\)GT.1943-5606.0001584](http://dx.doi.org/10.1061/(ASCE)GT.1943-5606.0001584) in press)
- 2) Vanmarcke, E.: Stochastic finite elements and experimental measurements, *Probabilistic Engineering Mechanics*, Vol. 9, pp.130-114 (1994)
- 3) Bruce L. K., Majid T. M., and Mourad Z.: Model Tests and Numerical Simulations of Liquefaction and Lateral Spreading, LEAP-UCD-2017, *Springer*, 2020
- 4) Vargas Tapia, R. R., Ueda, K. and Iai, S.: Effects of soil spatial variability on liquefaction behavior of horizontal layered ground, *Journal of Japan Society of Civil Engineerings*, Vol. 74, No. 4, I_16-I_24, 2018
- 5) Popescu, R., Prevost, J. H. and Deodatis, G.: Effects of spatial variability on soil liquefaction some design recommendations, *Geotechnique*, Vol. 47, No. 5, pp. 1019-1039, 1997
- 6) Popescu, R., Prevost, J. H. and Deodatis, G.: 3D effects in seismic liquefaction of stochastically variable soil deposits, *Geotechnique*, Vol. 55, No. 1, pp. 21-31, 2005
- 7) Iai, S., Matsunaga, Y. and Kameoka, T.: Space plasticity model for cyclic mobility, *Soils and Foundations*, Vol. 32, No. 2, pp. 1-15, 1992.
- 8) Nadim, F., Einstein, H. and RoBerds, W.: Probabilistic stability analysis for individual slope in soil and rock, *Proc. Int. Conf. on Landslide Risk Management*, pp. 63-98, 2005.
- 9) Shinozuka, M. and Deodatis, G.: Simulation of multi-dimensional Gaussian fields by spectral representation, *Applied Mechanics Reviews*, ASME, Vol. 49, No. 1, pp.29-53, 1996.

(Received)
(Accepted)